LIMNOLOGY and OCEANOGRAPHY

ASLO

Limnol. Oceanogr. 66, 2021, 3963–3975

doi: 10.1002/lno.11935

Removal of large viruses and their dispersal through fecal pellets of the appendicularian *Oikopleura dioica* during *Emiliania huxleyi* bloom conditions

Kyle Michael James Mayers,[1] **Janice Lawrence**,[2] **Katrine Sandnes Skaar**,[1] **Joachim Paul Töpper**,[3] **Elzbieta Petelenz**,[4] **Marius Rydningen Saltvedt**,[4] **Ruth-Anne Sandaa**,[4] **Aud Larsen**,[1,4] **Gunnar Bratbak**,[4] **Jessica Louise Ray**[1*]

[1]NORCE Norwegian Research Centre AS, NORCE Environment/Climate, Bergen, Norway
[2]Department of Biology, University of New Brunswick, Fredericton, New Brunswick, Canada
[3]Norwegian Institute for Nature Research (NINA), Bergen, Norway
[4]Department of Biological Sciences, University of Bergen, Bergen, Norway

Abstract

Despite their importance in shaping the structure and function of marine microbial food webs, little is known about factors regulating marine virus abundance. Previous work demonstrated clearance of laboratory-cultured *Emiliania huxleyi* virus by the appendicularian *Oikopleura dioica*; however, the applicability of this interaction to natural virus assemblages was not investigated. Here, we conducted controlled laboratory experiments using *O. dioica* and mesocosm water containing natural virus assemblages with high densities of virus, and measured removal of virus by *O. dioica* using both flow cytometry and molecular methods. Bayesian models based on flow cytometry quantification of virus particles demonstrated efficient removal of viruses (mean 90.3 mL ind^{-1} d^{-1}), with a clearance efficiency of 42.6% relative to food algae. Molecular detection of virus removal by quantification of viral *mcp* gene copies revealed a mean clearance rate of 68.1 mL ind^{-1} d^{-1}. Fecal pellets from these experiments demonstrated that viruses in fecal pellets retain infectivity despite passage through the *O. dioica* gut. Shotgun metavirome analysis demonstrated *O. dioica* removal of large virus groups, notably the Phycodnaviridae. The results demonstrate the removal of *E. huxleyi* virus from natural virus assemblages by *O. dioica* and the maintenance of viral infectivity when incorporated into fecal pellets, prompting further investigation on the fate of fecal-packaged viruses and their impact on host dynamics. Furthermore, our results indicate the generality of this interaction for other large algal viruses, raising questions about the implications of this mechanism of marine virus redistribution on the broader marine virus community.

Viruses are hugely abundant and richly diverse in the vast marine environment (Breitbart 2012; Breitbart et al. 2018). While there is a considerable body of evidence supporting the importance of marine viruses in the regulation of marine microbial diversity (Tarutani et al. 2000; Weinbauer and Rassoulzadegan 2004; Marston et al. 2012; Martiny et al. 2014) and function (Brussaard et al. 2008; Rohwer and Thurber 2009), a full understanding of the factors that regulate the abundance of marine virus populations in the water column is deficient (Thingstad 2000; Short 2012). Although virus decay (Noble and Fuhrman 1999 and references therein) and the sinking of infected host cells (Lawrence et al. 2002) are two mechanisms by which the abundance of some marine viruses are regulated, little is known about the general mechanisms of virus particle removal from the water column. A more complete understanding of virus removal factors (Mojica and Brussaard 2014) would contribute to more accurate estimates of the viral production rates required to offset these losses, and the net impact of viruses in the global ocean biosphere.

In a previous study, we demonstrated that the mesozooplankton *Oikopleura dioica* (Chordata: Tunicata) can efficiently

*Correspondence: jera@norceresearch.no

Additional Supporting Information may be found in the online version of this article.

Author Contribution Statement: J.L. and J.L.R. conceived and designed the incubation experiment, conducted the incubation experiment with logistical and technical assistance from K.M.J.M. J.L., K.M.J.M., E.P., K.S.S., H.M.S., and J.L.R. performed laboratory analysis. M.R.S. provided additional sample material. J.L., K.M.J.M., J.P.T., and J.L.R. analyzed results. J.L., K.M.J.M., and J.L.R. wrote the manuscript with contributions from A.L., J.P.T., G.B., M.R.S., and R.A.S.

remove the *Emiliania huxleyi* virus (hereafter referred to as "virus") from seawater during normal feeding in laboratory incubations (Lawrence et al. 2018). Despite the small size of virus particles (160–180 nm equivalent spherical diameter; Castberg et al. 2002), the intricate structure of the mucus net "house" that *O. dioica* uses to capture and concentrate food particles (Deibel and Powell 1987) enables it to efficiently remove the virus from seawater with clearance rates of 2–50 mL ind^{-1} d^{-1} (Lawrence et al. 2018). Furthermore, the detection of *E. huxleyi* virus DNA in the gut, discarded houses, and fecal pellets of *O. dioica* raises questions about the role of *O. dioica* feeding in the ecological trajectory of virus particles. The spatiotemporal coincidence of *O. dioica*, *E. huxleyi* and its virus in surface waters, in combination with the high potential flux of *O. dioica* houses (approx. 6–20 houses ind^{-1} d^{-1}) and fecal pellets (20–60 ind^{-1} d^{-1}), suggests that the removal and/or redistribution of virus particles by *O. dioica* may alter interactions between the virus and its host, with unknown consequences (González et al. 1994; Bratbak et al. 1995; Gorsky and Fenaux 1998; Sato et al. 2001; Båmstedt et al. 2005; Dagg and Brown 2005; Troedsson et al. 2007). Studies examining virus interactions with other nonhost macrofaunal organisms emphasize these interactions as important, but overlooked, virus removal factors in the marine environment (Frada et al. 2014; Welsh et al. 2020).

In June 2018, we were presented with the opportunity to obtain samples from an independent seawater mesocosm experiment designed to achieve a nutrient-induced *E. huxleyi* bloom with concomitant virus-induced bloom crash (Vincent et al. 2020). Capitalizing on this, we performed a clearance experiment with cultured *O. dioica* incubated in mesocosm seawater containing natural virus assemblages, including near bloom-peak densities of the *E. huxleyi* virus. This permitted us to assess the interaction between *O. dioica* and this virus in a mixed virus assemblage, as well as the fate of virus particles trapped in *O. dioica* fecal pellets. We proposed the following research questions:

1. Does *O. dioica* remove the virus from the mixed natural virus assemblages present at the peak of an *E. huxleyi* bloom?
2. Do virus particles trapped in *O. dioica* fecal pellets retain their infectivity?

We hypothesized that clearance by *O. dioica* of *E. huxleyi* virus in mixed natural virus assemblages would occur at rates similar to those observed for controlled laboratory clearance experiments (Lawrence et al. 2018). Furthermore, we hypothesized that some fraction of the virus particles passed in *O. dioica* fecal pellets would retain infectivity for host *E. huxleyi*, thus confirming the *O. dioica*–virus interaction as a potential mechanism for vertical redistribution of the virus in the marine environment. We discuss the possible implications of our findings in terms of the impact on viral ecology and the potential fates of viral particles within the marine environment.

Materials

Seawater mesocosms

A mesocosm experiment was conducted at the Espegrend Marine Biological Station (University of Bergen) from 22 May to 18 June 2018 (duration of 23 d). In brief, four 11 m^3 reinforced transparent polyethylene mesocosm bags (2 m diameter × 4 m depth) (Egge and Aksnes 1992) were filled with surrounding fjord water (Raunefjorden, 60.38°N; 5.28°E) from a depth of ~ 5 m by pump and left open to the atmosphere for the duration of the experiment. Circulation within bags was maintained using an AirLift system (Castberg et al. 2001). Inorganic nutrient additions were performed to stimulate a bloom of the coccolithophore *E. huxleyi* from the natural marine phytoplankton communities present at this site. Nitrate (1.6 μM $NaNO_3$) and phosphate (0.1 μM KH_2PO_4) were added on experimental days 0–5 and 14–17. In addition, nitrate alone (1.6 μM $NaNO_3$) was added on experimental days 6, 7, and 13. Cumulative nutrient additions were 20.8 μM nitrate and 1 μM phosphate.

Animal culturing

Cultures of *O. dioica* were obtained from the Appendicularian Facility at the Sars International Centre for Marine Molecular Biology at the University of Bergen. One day post-spawn cultures were transferred to the Espegrend Marine Biological Station and maintained in a climate-controlled culturing facility according to established methods (Bouquet et al. 2009). All culture maintenance and experimental incubations were conducted at 14°C, at which the generation time of *O. dioica* is approx. 6 d. As previous clearance experiments using *O. dioica* and the *E. huxleyi* virus with the same culturing conditions demonstrated maximum virus clearance by 5-d-old (D5) *O. dioica* animals (Lawrence et al. 2018), D5 animals were used for the present study.

Clearance experiment design

To assess virus removal from natural virus assemblages, *O. dioica* was incubated in water collected from mesocosm bags around the time of the *E. huxleyi*/*E. huxleyi* virus bloom peak (experimental day 18, 11 June 2018) when virus density was ~ 2×10^7 mL^{-1} (Vincent et al. 2020). Six liters of water from each of four mesocosm bags (M1–M4) were collected and pooled. This 24-liter pooled water sample was prefiltered through a 10-μm nitex mesh prior to serial filtration through a 3-μm polycarbonate and GF/F filters (Whatman) (142-mm diameter) to remove all potential host phytoplankton cells (host-free water). A previous study determined the equivalent spherical diameter of *E. huxleyi* to be 4.7 μm (Hansen et al. 1996), therefore we chose 3-μm filters in combination with GF/F filters (effective pore size 0.7 μm) to remove

nanophytoplankton cells, including *E. huxleyi*, from incubation water while allowing viruses to pass through. Four liters of host-free water were dispensed into each of six 8-liter polycarbonate beakers (Bouquet et al. 2009), three of which were randomly chosen to serve as experimental beakers, while the remaining three served as control beakers (see below). Temperature and salinity of host-free water were determined to be 16°C and 30.3 ppm, respectively. *Isochrysis galbana* was added at a final concentration of 8000 cells mL^{-1} as food algae to all six beakers. Developmental stage D5 *O. dioica* animals were gently transferred by wide-bore pipette into the three experimental beakers to achieve a density of 20 *O. dioica* individuals per liter (Lawrence et al. 2018). The remaining three beakers were kept without animal addition to serve as negative control experimental incubations. The start of the clearance experiment (T0) was set to 30 min after the completion of animal transfer to allow animals to recover from transfer stress and commence normal feeding. All incubations, including negative controls, were kept at constant temperature (14°C) with gentle stirring (Bouquet et al. 2009). Beakers were visually monitored for sexually mature (nonfeeding) individuals, which were immediately removed by gentle pipetting to avoid spawning and replaced with a fresh D5 animal from a maintenance culture. Animal replacement was completed within 1.5 h of the start and did not result in the replacement of more than 10% of the initial population (data not shown). Water samples were collected hourly to estimate virus abundance using different methods (see the "Estimating virus abundance" section) for a total of 8 h. Samples are referred to by sampling time in hours, with "T0" samples taken at the start of the experiment and "T8" samples taken at the end of the experiment. At the conclusion of the experiment (T8), the remaining incubation water was sampled to analyze virus assemblages using shotgun metavirome sequencing and pulsed-field gel electrophoresis (PFGE; see the "Virus assemblage diversity" section). In addition, *O. dioica* fecal pellets were collected for *E. huxleyi* infection assays (see the "Infectivity of *E. huxleyi* virus in *O. dioica* pellets" section).

Estimating virus abundance

Two methods were employed to measure virus abundance in water from experimental incubations—flow cytometry and droplet digital polymerase chain reaction (PCR). These methods measure, respectively, free virus particles and virus genome equivalents.

Flow cytometry

At hourly intervals from T0 to T8, triplicate 0.5-mL samples of water were collected from incubation beakers by careful pipetting to avoid aspiration of animals, discarded houses, and visible particulate debris. Samples were fixed with 0.5% (v/v) glutaraldehyde, mixed thoroughly by gentle inversion, and incubated for 30–120 min at 4°C in the dark. Samples were then flash frozen in liquid nitrogen and transferred to −80°C storage until analysis. Fixed samples were thawed and divided into two aliquots for counting (1) phytoplankton cells or (2) viruses. For phytoplankton counts, undiluted fixed samples were run directly on an Attune NxT Flow cytometer for 1.5 min each using a flow rate of 100 μL min^{-1} and triggering on chlorophyll *a* (Chl *a*) autofluorescence (695/40, further referred to as BL3). The food algae *I. galbana* was gated according to BL3 plotted against side scatter using the Attune NxT software v2.7.0. For viral flow cytometry counts, appropriate sample dilutions were prepared with 0.2 μm-filtered 1X TE (10 mM Tris-Cl, 1 mM EDTA, pH 8.0) buffer containing 1X SYBR Green I nucleic acid stain (Thermo Fisher Scientific). Dilutions were heated to 80°C for 10 min and then equilibrated to room temperature in the dark before counting on a FACSCalibur flow cytometer (BD Biosciences) as described previously (Lawrence et al. 2018). *E. huxleyi* virus was readily distinguishable from other large viruses (Fig. S1).

Droplet digital PCR (ddPCR)

We sampled for droplet digital PCR analysis only at T0 and T8 in order to maximize the time elapsed between samples and thereby reduce the signal from free virus DNA in the incubation water (Lawrence et al. 2018). Aliquots of incubation water (1 mL) were sampled from each beaker by careful pipetting, and immediately frozen at −20°C. Prior to DNA extraction, frozen samples were thawed, and a 0.5-mL subsample was removed for DNA extraction and droplet digital PCR analysis. The unused sample volume was returned to −20°C storage. Lysis of virus particles in subsamples was performed by heating at 90°C for 1 min immediately followed by chilling on ice for 1 min. DNA was then extracted using the DNeasy Blood & Tissue mini kit (QIAGEN) according to the manufacturer's protocol. DNA was eluted with 100 μL Buffer EB (QIAGEN) and stored at −20°C until analysis.

Details regarding primer modification and assay optimization are available in the Supplementary Information. Droplet digital PCR reactions were run with a total volume of 20 μL on a DX200 instrument (Bio-Rad Laboratories) using 5 μL template DNA, 1X EvaGreen Supermix (Bio-Rad Laboratories), 250 nM (final concentration) of primers MCP1Fw (5′-ACGC ACCCTCAATGTATGGAAGG-3′) (Pagarete et al. 2009) and MCP94RvMOD (5′-RTSCRGCCAACTCAGCAGTCGT-3′) (see Supplementary Information for detailed information), and ultrapure water. Negative (no template) controls and positive controls contained, respectively, ultrapure water or purified DNA from virus strain EhV-99B1, as template, and were included in all droplet digital PCR runs. Assay sensitivity was confirmed using agarose gel electrophoresis (Fig. S2). PCR reactions were emulsified with QX200 Droplet Generation Oil for EvaGreen in 8-tube PCR strips (Bio-Rad Laboratories) using the QX200 Droplet Generator (Bio-Rad Laboratories), then gently transferred by multichannel pipette into a droplet digital PCR 96-well plate (Bio-Rad Laboratories). Plates were sealed with pierceable sealing foil (Bio-Rad Laboratories) using a PX1

PCR plate sealer (Bio-Rad Laboratories). 96-well PCR reactions were performed in a C1000 Touch thermocycler with deep-well module (Bio-Rad Laboratories) using the following program: 95°C for 5 min; 40 cycles of 95°C for 30 s then 62°C for 1 min; 4°C for 5 min; 90°C for 10 min; 10°C infinite hold. Plates were allowed to equilibrate to room temperature for at least 15 min prior to analysis using the QX200 Droplet Reader (Bio-Rad Laboratories). Thresholds for positive/negative droplet separation were manually set according to results from negative controls.

Clearance rate calculations

Clearance rates based on flow cytometry counts were calculated for both *I. galbana* and the virus similarly to Lawrence et al. (2018). In brief, clearance rate intervals were calculated using posterior clearance distributions calculated from hierarchical linear models with normal errors under Bayesian inference using the R-package "rjags" (Plummer 2016) as described previously (Lawrence et al. 2018). The main difference in this study was the use of one control treatment for background loss processes such as viral decay. The posterior from the control treatment was subtracted from the posterior of the *O. dioica* treatments to calculate clearance rates. For virus only, clearance rates based on droplet digital PCR results were also calculated using the same model. The start (T_{START}) and end (T_{END}) time points for clearance rate calculations from flow cytometry results were chosen based on the time window for linear *I. galbana* removal during incubations with *O. dioica*. Accordingly, T3 and T8 were chosen as start and end points, respectively, for clearance rate calculations from flow cytometry results for *I. galbana*, the *E. huxleyi* virus, and other large viruses. For droplet digital PCR results, clearance rates for virus were calculated using T0 as start and T8 as end points in order to maximize time elapsed (see above).

Viral assemblage diversity

Shotgun metavirome sequencing

For shotgun metavirome analysis, duplicate 50-mL water samples from each beaker were collected at T0 and T8, and serially filtered through 52- and 10-μm nitex mesh followed by a GF-C filter mounted in a 25-mm diameter Swinnex filter holder. Filtrates were stored in the dark at 4°C for up to 48 h prior to ultracentrifugation for 2 h at 14,100 × *g* and 10°C (Sandaa et al. 2001). Virus pellets were stored at −20°C until DNA extraction. Frozen virus pellets were heated to 90°C for 1 min and then rapidly chilled on ice for 1 min to break open viral capsids. DNA was extracted using a QIAsymphony SP instrument (QIAGEN) with the DSP DNA mini kit (QIAGEN) and Tissue_LC_200_V7_DSP protocol (QIAGEN). Purified DNA was eluted in 50 μL and stored at −20°C. Metavirome libraries were generated using the Nextera XT library preparation kit (Illumina) following the manufacturer instructions and using 1–5 ng viral DNA as input. One sample (control beaker 3, T8) failed the library preparation and was therefore not sequenced. Sequencing library concentration and size distribution were assessed using the Agilent Bioanalyzer (High Sensitivity DNA assay kit) and libraries were subsequently pooled at equimolar concentrations. High-throughput sequencing was carried out using Illumina HiSeq 1500 (2 × 250 bp, paired-end) in Rapid mode at the CeBiTec Center for Biotechnology, Genomics Platform, at the Universität Bielefeld (Bielefeld, Germany). Bioinformatic analysis was conducted by the CeBiTec Computational Metagenomics group at Universität Bielefeld. Briefly, raw reads were quality-trimmed using Trimmomatic v0.3.5 with a sliding-window approach (window size: 4; quality threshold: 30) (Bolger et al. 2014). Based on results from a comparison of different metagenome assemblers for complex community analysis (Sczyrba et al. 2017), MEGAHIT v1.1.1 was used for metavirome assemblies in meta-sensitive mode (Li et al. 2015). Gene calling was conducted using Prodigal (Hyatt et al. 2010) and DIAMOND (Buchfink et al. 2015) searches against the NCBI non-redundant (nr) database (NCBI Resource Coordinators 2016). MEGAN (Huson et al. 2007) was used to determine the taxonomy of DIAMOND hits against the nr database. Assembly yielded approximately 1.5 Gbp of assembled sequence data distributed across 13 samples (Table S1). Raw metavirome sequences are publicly available as BioProject PRJNA682926.

Pulsed-field gel electrophoresis

Detailed information about preparation and analysis of PFGE samples is available in the Supplementary Information. In brief, all remaining incubation water from each treatment (control or *O. dioica*) at the end of the experiment (T8) was pooled by treatment (approx. 12 L per treatment) and serially prefiltered through 52- and 10-μm nitex mesh. Filtrates were stored at 4°C for a maximum of 16 h prior to filtration through 0.2-μm polycarbonate filters (Whatman) to remove cells and cellular debris. An additional virus concentration step with tangential flow filtration as described previously (Sandaa et al. 2018) reduced sample volume to ~ 50 mL (~ 240-fold concentration). PFGE was performed as described in Johannessen et al. (2015). Briefly, ultracentrifuge-concentrated viruses were lysed and electrophoresed in 1X TBE buffer at 14°C in a pulsed field electrophoresis chamber (Amersham Biosciences) at 6 V cm^{-1} for 22 h with pulse ramps from 20 to 40 s. Bands of interest were excised from the gel using a sterile scalpel and stored individually at −20°C until DNA recovery by electro-elution using a 10 kDa dialysis tube (Spectrum Laboratories) immersed in 1X TAE buffer (20 mM Tris-Cl, 20 mM acetic acid, pH 8.0) (Supplementary Information).

Infectivity of E. huxleyi *virus in* O. dioica *fecal pellets*

An aliquot of filtered mesocosm water was sampled to measure the background abundance of infectious virus particles in the incubation water using a most probable number assay with *E. huxleyi* 374 as host, confirming our ability to detect infectious virus particles from mesocosm water (Supplementary Information). *O. dioica* fecal pellets from control incubations were

collected by gentle pipetting from the bottom of D5 *O. dioica* maintenance cultures using a sterile serological pipette. Fecal pellets from mesocosm water incubations with *O. dioica* were collected from the 10-μm nitex mesh used to prefilter the T8 clearance incubation water for PFGE. Fecal pellets collected on the plankton mesh were gently washed into sterile 50 mL Falcon tubes using ultra-filtered (filtrate from tangential flow filtration, 100 kDa) seawater. Fecal pellets were stored at 4°C in the dark and assayed within 72 h of collection. Fecal pellet samples were decanted onto 10-μm mesh, thoroughly but gently rinsed using ultra-filtered seawater, and then transferred to fresh ultra-filtered seawater in a sterile petri dish. Single fecal pellets were micropipetted into microtiter plate wells (24 fecal pellets from control incubations and 48 fecal pellets from mesocosm water incubations). To each well, 140 μL of exponentially growing *E. huxleyi* (CCMP 374) was added for a final density of 10^5 cells mL^{-1}. Microtiter plates were incubated at 16°C with 50 μm photons m^{-2} s^{-1} and a 14:10 light/dark regime for 6 d prior to analysis by plate reader (Enspire, PerkinElmer) for relative Chl *a* fluorescence. Positive lysis was scored as at least one order of magnitude (90%) decrease in fluorescence relative to controls.

Results

Clearance rates

The food alga *I. galbana* initially increased in abundance from ~ 3.6×10^3 cells mL^{-1} at T0 to ~ 6.0×10^3 cells mL^{-1} at T3 in both control and *O. dioica* treatments. After this initial increase, *I. galbana* in the *O. dioica* treatment decreased in a linear fashion until T8, at which point 1.5×10^3 cells mL^{-1} remained (Fig. 1A). In control incubations without *O. dioica*, the density of *I. galbana* continued to increase, peaking at 1.1×10^4 cells mL^{-1} at T7 and subsequently decreasing to 8.5×10^3 cells mL^{-1} by T8 (Fig. 1A). Starting (T0) densities of virus particles (determined by flow cytometry as shown in Fig. S1) in both treatments ranged from 4.5–9.4 $\times 10^5$ particles mL^{-1} (Fig. 1B). For the *O. dioica* incubations, we observed an initial increase in the virus from T0 to T1, which was followed by a gradual decrease until the end of the experiment, except for a slight increase at T5 (Fig. 1B). Final virus counts in the *O. dioica* treatment were 2.7–3.9 $\times 10^5$ particles mL^{-1}. In control incubations, virus counts decreased from T0 to T3 and then increased and remained stable until T8, with a final concentration of 6.1–7.6 $\times 10^5$ particles mL^{-1} (Fig. 1B).

Using flow cytometry counts of *I. galbana* as reference, we determined that the period of linear clearance by *O. dioica* occurred between T3 and T8 (Fig. 1A). This time period was subsequently chosen for the calculation of clearance rates for both *I. galbana* (Fig. 1C) and the virus (Fig. 1D). Model diagnostics confirm successful model convergence, adequate predictive power and homoscedasticity of errors and are available in the Supplementary Information (Fig. S3). The mean clearance rate for *I. galbana* was 212.1 mL individual^{-1} d^{-1} (141.1–283.2 mL ind^{-1} d^{-1} with 95% credible intervals) (Fig. 1C), and

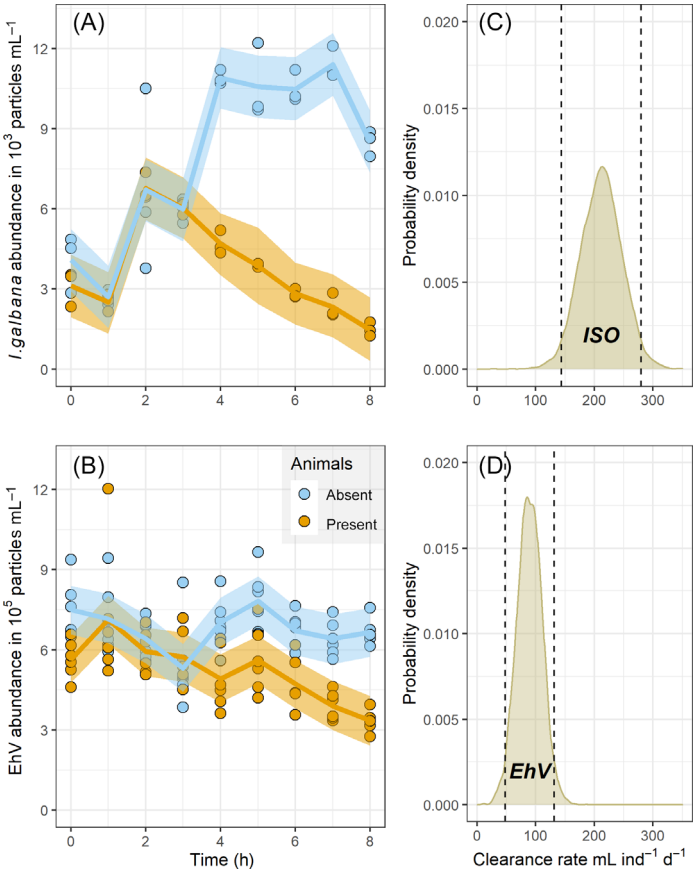

Fig. 1. Flow cytometric detection of clearance by *O. dioica*. Counts of (**A**) *I. galbana* (10^3 cells mL^{-1}) and (**B**) *E. huxleyi* virus (10^5 particles mL^{-1}) in experimental incubations. Blue circles and curves indicate control incubations without *O. dioica*; yellow circles and curves indicare experimental incubations with *O. dioica*. Shaded regions represent 95% confidence intervals. Density plot of posterior distributions of flow cytometric clearance rate calculations (mL individual^{-1} d^{-1}) for (**C**) *I. galbana* and (**D**) the virus (EhV). Probability density (y-axis) shows the relative likelihood of given clearance rate values. Dashed vertical lines indicate 95% credible intervals.

for the virus was 90.3 mL ind^{-1} d^{-1} (46.1–130.6 mL ind^{-1} d^{-1}) (Fig. 1D). Setting the clearance efficiency of *I. galbana* at 100%, relative clearance efficiency of the virus by *O. dioica* was 42.6%. An additional large virus population distinct from the *E. huxleyi* virus was identified in flow cytograms (Fig. S1). From the same flow cytometry data, we were able to measure dynamics in the different experimental treatments (Fig. S4A) and calculate clearance rates (Fig. S4B) of this unidentified large virus-like particle. Clearance rates using the same T3–T8 time window were determined to be 48.5 mL ind^{-1} d^{-1} (7.1–87.9 mL ind^{-1} d^{-1}) (Fig. S4B), resulting in a clearance efficiency relative to *I. galbana* of 22.9%.

Molecular quantification using droplet digital PCR of *E. huxleyi* virus genome equivalents from T0 and T8 samples from both control and *O. dioica* treatments yielded positive detection in all experimental samples (Fig. S5A). Generality of

the assay for detection of a diversity of *E. huxleyi* viruses was confirmed by successful droplet digital PCR detection of cultured isolate EhV-99B1 (Castberg et al. 2002), mesocosm water sampled at the end of the mesocosm experiment after the virus peak, and *E. huxleyi* virus strains isolated at the end of the mesocosm experiment (Fig. S5B). The specificity of the droplet digital PCR assay for specific detection of *E. huxleyi* viruses was confirmed by unsuccessful detection of the commonly co-occurring viruses *Chrysochromulina ericina* virus (CeV), *Micromonas pusilla* virus (MpV), and *Phaeocystis pouchetii* virus (PpV) (Fig. S5B). The number of viral *mcp* gene copies in the control treatments decreased from $4.0 \pm 1.2 \times 10^4$ gene copies mL^{-1} (mean ± SD) to $3.6 \pm 0.5 \times 10^4$ gene copies mL^{-1} from T0 to T8 (Fig. 2A. In contrast, the *O. dioica* treatment resulted in a significant net decrease in viral *mcp* gene copy numbers from $4.6 \pm 0.9 \times 10^3$ copies mL^{-1} at T0 to 1.9 ± 0.2 copies mL^{-1} at T8 (two-tailed paired *t*-test, $p = 0.04$, $n = 6$). Using the same model for calculation of clearance rates from flow cytometry counts, we calculated mean clearance rate from droplet digital PCR quantification of viral *mcp* gene copies in the *O. dioica* treatment to be 68.1 mL ind^{-1} d^{-1} (18.0–120.8 mL ind^{-1} d^{-1}) (Fig. 2B).

Virus assemblage diversity

Shotgun metavirome analysis of virus fractions from T0 and T8 incubation water with or without *O. dioica* generated 222,648,188 paired end reads, of which 199,794,542 (10.2%) passed quality-trimming (Table S1) to yield 141,742–392,536 total reads per sample, with virus reads comprising 21,766–65,299 reads per sample. Proportionally, the virus fraction represented 13.06%–16.83% of total reads per sample (Fig. 3). Comparisons of changes in proportional virus group abundances from T0 to T8 for control incubations (Fig. 3, "absent") and *O. dioica* incubations (Fig. 3, "present") revealed a trend toward increased removal of some large double-stranded DNA virus groups when *O. dioica* were present (Fig. 3). Wilcoxon rank sum tests of proportional metavirome read count removal from T0 to T8 identified a significant effect of *O. dioica* on removal of Mimiviridae (family-level) and Unclassified Phycodnaviridae (genus-level) (Fig. 3; Table 1). Removal by *O. dioica* of Coccolithovirus reads, the viral genus which includes the *E. huxleyi* virus, was not significant (Fig. 3; Table 1).

PFGE analysis of dsDNA virus genomes present in T8 control incubations revealed approximately 15 bands ranging in size from less than 48.5 kb to greater than 533.5 kb (Fig. 4). One band at ~ 400 kb (arrow in Fig. 4) is in the same size range as the draft genome sequence for *E. huxleyi* virus isolate EhV-163 (Allen et al. 2006) and other *E. huxleyi* virus isolates (Pagarete et al. 2014) observed during mesocosm experiments conducted at the same site in 2000 and 2008, respectively.

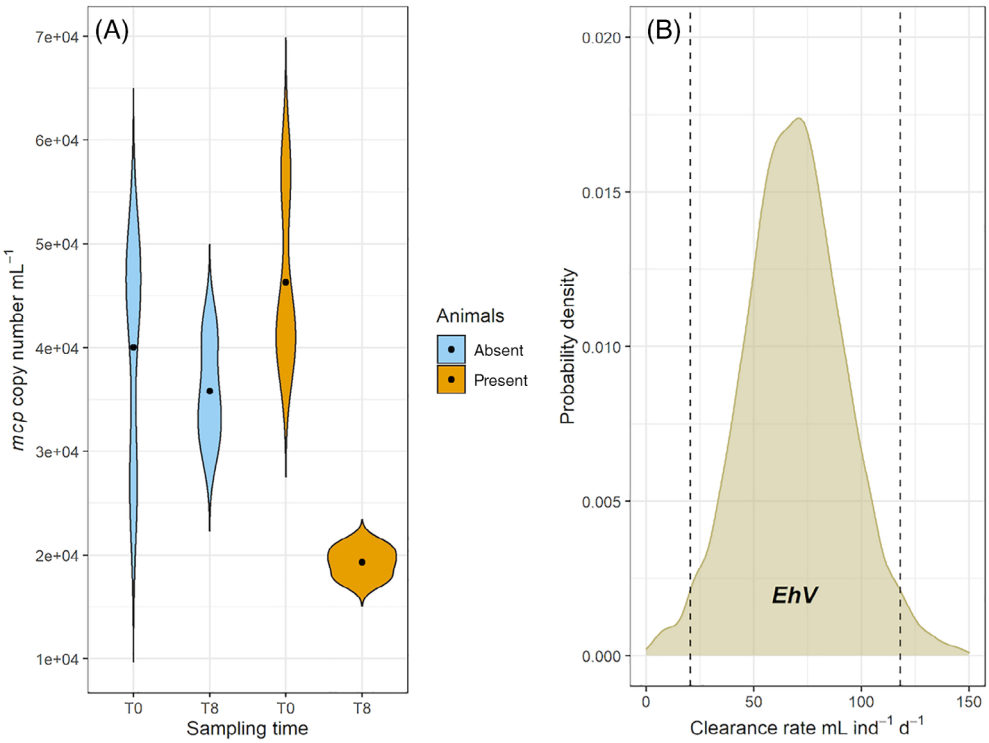

Fig. 2. Molecular detection of *Emiliania huxleyi* virus clearance by *O. dioica*. (**A**) Violin plot showing triplicate droplet digital PCR measurements of viral *mcp* gene copies (10^4 mL^{-1}, y-axis) in virus pellets from control (blue) and *O. dioica* (yellow) incubations. Sampling time in hours in shown on the x-axis. Black points show mean values. (**B**) Clearance rate calculations of removal of virus by *O. dioica* using droplet digital PCR measurements of viral *mcp* gene copies mL^{-1}. Dashed vertical line indicates 95% credible intervals.

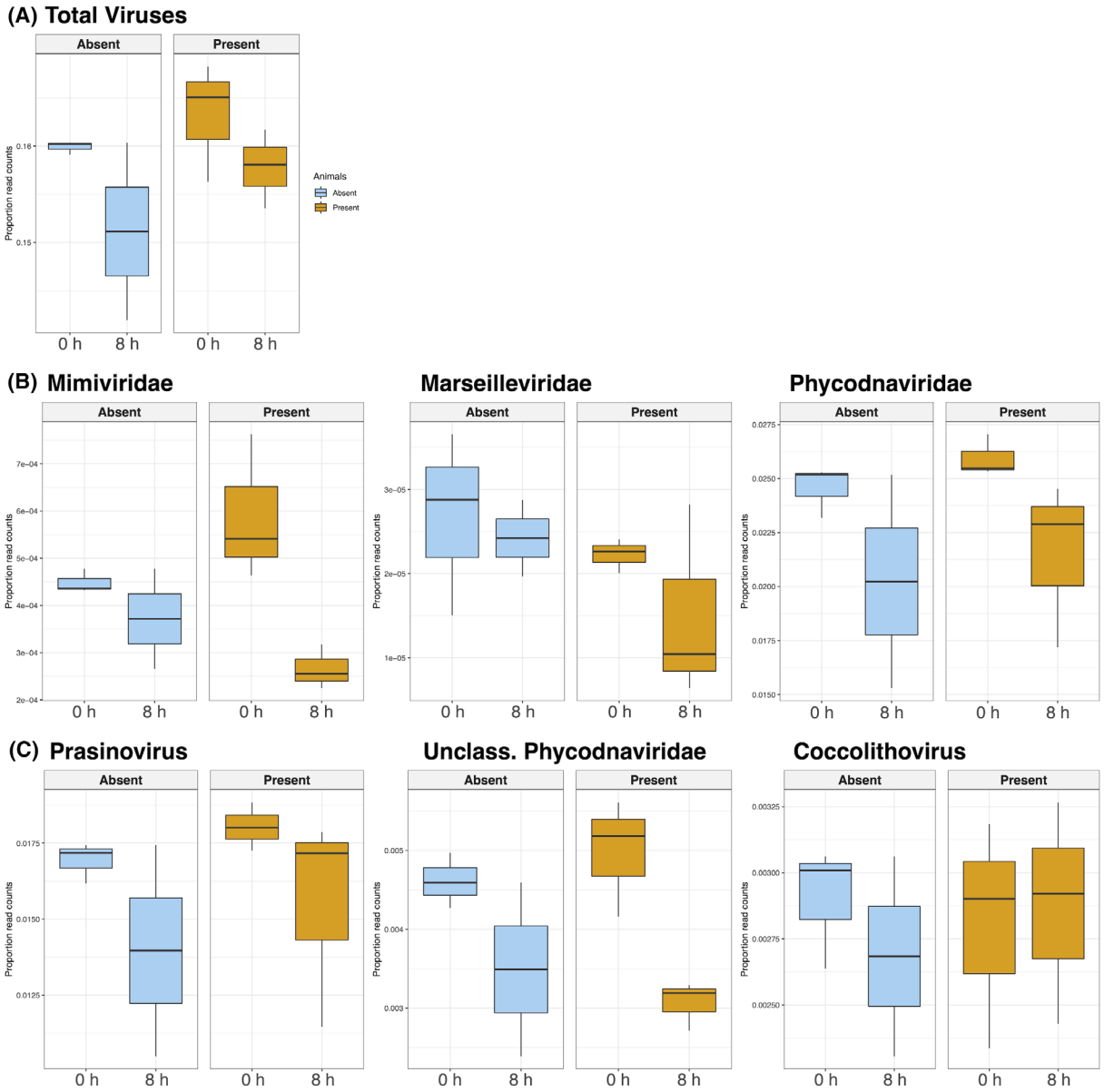

Fig. 3. Shotgun metavirome analysis of T0 and T8 virus fractions from clearance experiment with *Oikopleura dioica*. Boxplots show abundance-normalized read counts (proportion of read counts) for each taxonomic ranking (**A**) kingdom, (**B**) family, and (**C**) genus/species from triplicate clearance experiments incubated in the presence (present) or absence (absent) of *O. dioica*. Color designation shown in legend for A applies also to B and C.

A BLAST search of the *mcp* sequence amplified from electro-eluted DNA from this band (Supplementary Information) using *E. huxleyi* virus-specific *mcp* primers (Schroeder et al. 2002) revealed 100% sequence similarity (274/274 identities) to virus clone OTU-52 (Accession number GU936230.1), and 97.18% identity with 100% coverage to the draft genome sequence of EhV-99B1 (Accession number FN429076.1), confirming the *E. huxleyi* virus as the origin of this pulsed field gel band. Incubations with *O. dioica* demonstrated complete visual loss of bands in the size range 97 to > 533.5 kb, including the *E. huxleyi* virus band at ~ 400 kbp.

Fate of ingested viral particles

After 6 d of incubation, lysis of host *E. huxleyi* occurred in only 1 of 24 wells containing *O. dioica* fecal pellets from maintenance cultures (negative control). In contrast, lysis of *E. huxleyi* was observed in all 48 wells to which single fecal pellets from the mesocosm-water feeding *O. dioica* were added.

Discussion

Previous work demonstrated clearance of a cultured *E. huxleyi* virus by *O. dioica* under controlled laboratory

Table 1. Wilcoxon rank sum tests (W) to identify significant changes from T0 to T8 in the abundance-normalized large virus metavirome counts in clearance experiment incubation water. Treatment indicates whether incubations occurred in the presence ("present") or absence ("absent") of *O. dioica*. Tests were performed at different taxonomic ranks ("taxon"). Significant *p*-values are shown in bold.

O. dioica treatment	Taxon	W	*p*-value
Present	Total viruses	13	0.2000
	Marseilleviridae	8	1.0000
	Mimiviridae	16	**0.0286**
	Phycodnaviridae	14	0.1143
	Prasinovirus	13	0.2000
	Unclassified Phycodnaviridae	16	**0.0286**
	Coccolithovirus	7	0.8857
Absent	Total viruses	9.5	0.2845
	Marseilleviridae	8.5	0.4755
	Mimiviridae	9.5	0.2845
	Phycodnaviridae	9.5	0.2845
	Prasinovirus	8.5	0.4755
	Unclassified Phycodnaviridae	9.5	0.2845
	Coccolithovirus	6.5	1.0000

settings (Lawrence et al. 2018). The present study was conducted to expand on these findings and investigate this interaction and its implications using communities of marine viruses naturally enriched in this virus. A mesocosm experiment targeting *E. huxleyi* bloom dynamics provided the ideal opportunity to test virus removal rates by *O. dioica* when the *E. huxleyi* virus was one of many marine viruses present in a natural mixed virus assemblage. Our main focus was on clearance of the virus by *O. dioica*; however, viral community analyses (shotgun metavirome sequencing and PFGE) were also applied in order to facilitate a more general, qualitative assessment of the impact of *O. dioica* feeding on the broader double-stranded DNA virus assemblage. Our results show that the virus is efficiently cleared by *O. dioica* at rates that are comparable with clearance rates established using laboratory clearance experiments (Lawrence et al. 2018). Furthermore, demonstrating the removal of other large double-stranded DNA viruses by *O. dioica* using shotgun metagenome analysis of virus assemblages widens the potential implications for this interaction in natural marine femtoplankton assemblages. Finally, we have demonstrated that *O. dioica* grazing on the *E. huxleyi* virus results in the packaging of infectious virus particles into *O. dioica* fecal pellets, and that these particles are able to transmit infection to surrounding *E. huxleyi* cells. These findings thus provide new knowledge about the role of the *O. dioica–E. huxleyi* virus interaction in regulating the fate of this virus in the marine environment.

The removal of marine viruses by micro- and mesozooplankton in the marine environment is understudied, as evidenced by the paucity of investigations targeting such nonhost interactions. In addition to *O. dioica* (Lawrence et al. 2018), there are indications that copepods (Frada et al. 2014) and phagotrophic nanoflagellates (González and Suttle 1993) can feed directly on planktonic viruses, albeit with minimal contribution to nutrition. A recent investigation of the ability of both zooplankton and benthic fauna revealed the surprising ability of many macroorganisms to significantly reduce the abundance of a large virus in controlled seawater incubations (Welsh et al. 2020). The intricate feeding mechanics of filter-feeding macrofauna are optimized for small particle retention (Flood 1978; Bedo et al. 1993; Fernández et al. 2004; Sutherland et al. 2010), and we anticipate that further research will expand not only the scope of nonhost plankton interactions with marine viruses, but also the downstream impact of these interactions on existing models of virus-mediated regulation of host diversity and abundance (Martiny et al. 2014) and nutrient turnover (Rohwer and Thurber 2009) in the ocean.

Clearance rates for the virus measured in this study (90.3 mL ind^{-1} d^{-1}) were higher than those previously reported for the same virus (~ 45 mL ind^{-1} d^{-1}) (Lawrence et al. 2018). This is likely due to the calculation of the clearance rate from the time window for linear virus removal by *O. dioica*, that is, T3–T8 (Fig. 1), in the present study. The clearance rate for *I. galbana* by *O. dioica* in this study using animals with trunk length of 0.96 ± 0.15 mm were comparable to published estimates for similarly sized animals (Broms and Tiselius 2003), indicating that animals were feeding normally during the experiment. It is noteworthy that clearance rates calculated from droplet digital PCR quantification of virus genome equivalents (Fig. 2) are consistently lower than clearance rates based on flow cytometry counts (Fig. 1) from the same experiment. One possible explanation is that viral DNA is released into incubation water as virus particles lyse naturally, or are ingested and defecated by *O. dioica*, during incubations, resulting in lower apparent "removal" of virus genome equivalents and, hence, lower clearance rates. This free viral DNA would not affect flow cytometry analysis as the latter methodology detects particles only (i.e., DNA packaged in capsids). Enzymatic treatment of sampled water to selectively remove free viral DNA, and thereby determine the relative contribution of free vs. encapsulated viral DNA to droplet digital PCR signal, may provide new information about the observed discrepancy between flow cytometry and molecular quantification results.

Using shotgun metavirome sequence analysis of T8 incubation water virus fractions, we were able to detect significant removal of Mimiviridae (family rank) and Unclassified Phycodnaviridae (genus rank) (Table 1) in *O. dioica* incubations, an effect that was not observed in the control treatment (Table 1). Although these two viral groups encompass important and ecologically distinct viruses in the marine environment (Wilson et al. 2009; Johannessen et al. 2015; Claverie and Abergel 2018), metavirome analysis did not demonstrate

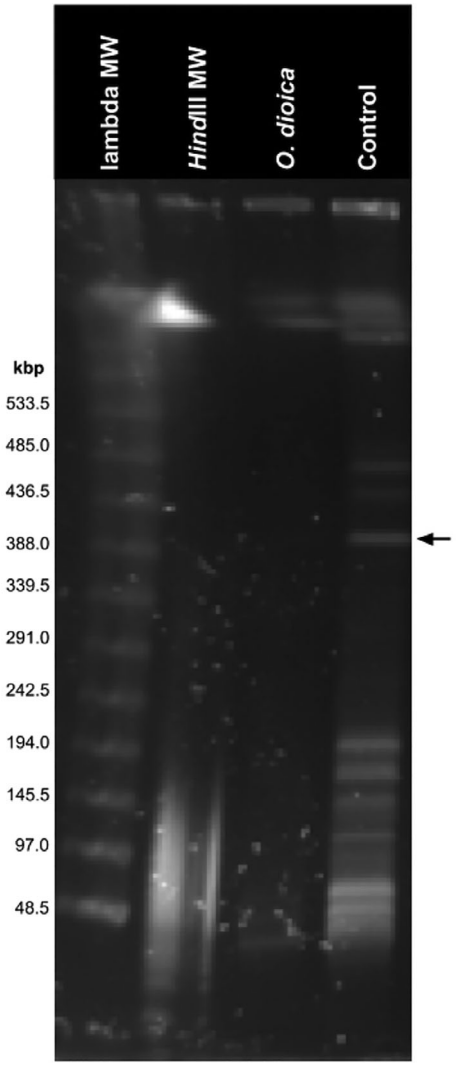

Fig. 4. Pulsed field gel electrophoretic separation of concentrated and pelleted double-stranded DNA virus genomes from incubation water at the end (T8) of clearance incubations. See the "Materials" section for a description of virus pellet preparation for pulsed field gel electrophoresis. Lane designations from left are: Lane 1 – lambda molecular weight (MW) standard, with MW indicated in kilobase pairs (kbp); lane 2 – *Hind*III digest of the MW standard; lane 3 ("*O. dioica*") – double-stranded DNA virus genome diversity from pooled triplicates of mesocosm water (12-liter total volume) after incubation for 8 h in the presence of *O. dioica*; lane 4 ("control") – double-stranded DNA virus genome diversity from pooled triplicates of mesocosm water (12-liter total volume) after incubation for 8 h in the absence of *O. dioica*. The black arrow on the right side of the figure indicates an *Emiliania huxleyi* virus band at approximately 400 kbp.

the removal of Coccolithoviruses (Fig. 3; Table 1), which should include *E. huxleyi* virus. These results are therefore in disagreement with the clearance rate results from flow cytometry (Fig. 1) and droplet digital PCR (Fig. 2) analyses. The reason why removal of unclassified Phycodnaviridae, but not specifically Coccolithovirus, could be demonstrated is unknown. One possible explanation is that sequence diversity within the *E. huxleyi* virus assemblages present in incubation water obscured genus-level classification as Coccolithovirus.

PFGE results (Fig. 4) showed complete removal of a diversity of large double-stranded DNA viruses down to ~ 100 kbp, including the *E. huxleyi* virus band at ~ 400 kbp. This contrasts with results from flow cytometry (Fig. 1) and droplet digital PCR (Fig. 2), which indicate significant, but only partial, clearance of the virus by *O. dioica*. According to flow cytometry counts (Fig. 1), approx. 3×10^5 virus particles mL^{-1} remain at T8 when water was sampled for PFGE. Assuming a viral genome size of 402,500 bp (Allen et al. 2006) and a DNA molecular weight of 650 g mol^{-1}, the remaining genetic signal from 3×10^5 virus particles mL^{-1} would amount to 130 pg viral DNA mL^{-1} in incubation water. As 12 liters of incubation water was pooled and concentrated for PFGE, this would scale up (130 pg $\times$ 12,000 mL) to approximately 1.56 μg of *E. huxleyi* virus DNA in the agarose plugs used for PFGE. Taking into consideration the DNA contribution from all other viruses (i.e., the other gel bands) present in T8 incubation water would further increase the total DNA concentration in agarose plugs. Allowing for considerable (10%–90%) loss of the virus during sample preparation for electrophoresis due to inevitable inefficiency of filtration and concentration steps, this would still result in tens to hundreds of nanograms of *E. huxleyi* virus DNA in one electrophoresis sample, a concentration that is strongly in excess of reported minimum values for double-stranded DNA detection (~ 34 pg) in agarose gels using the SYBR Gold stain (Tuma et al. 1999). We must therefore treat the quantitative value of our PFGE result for virus removal by *O. dioica* with caution. The most likely explanation for the complete removal of viruses > 100 kbp is the large quantity of discarded *O. dioica* houses, fecal pellets, and other particulates present in T8 incubation water. This accumulated material likely formed a mat on the 52 and 10 μm mesh used to prefilter the incubation water which removed viruses > 100 kb (Supplementary Information). Interestingly, any such filtration effect is congruent with our conceptual model that *O. dioica* houses efficiently trap large algal viruses.

Our study supports some degree of size selectivity by *O. dioica* for particle removal, although we cannot conclude the primacy of size selection for removal of marine viruses by *O. dioica*. In a study of *O. dioica* clearance rates using synthetic spherical and ellipsoid particles, Conley and Sutherland (2017) showed that particle shape affected the efficiency of trapping and ingestion. It is also possible that differences in particle properties due to, for example, the presence of an external lipid membrane (Qin et al. 2001; MacKinder et al. 2009; Martínez-Martínez et al. 2015), net charge (Rao et al. 1986), hydrophobicity (Dadon-Pilosof et al. 2017), or other abiotic parameters, may affect the likelihood of a virus being trapped in an *O. dioica* house. Indeed, marine viruses are represented by a diversity of sizes and morphologies (Brum et al. 2013), both of which may affect the likelihood and/or efficiency of their interaction with *O. dioica*.

The lysis of cultures incubated with fecal pellets shows that *O. dioica* fecal pellets contain infectious virus particles, and that these particles become available to infect surrounding host *E. huxleyi* cells, albeit at unknown rates. As complete culture lysis was observed within 6 d after adding fecal pellets, and the infectious cycle of the virus is estimated at 24–48 h (Mackinder et al. 2009), our results clearly support some degree of shedding of infectious virus particles from fecal pellets, despite pellets remaining intact. Our most probable number estimates of infectious virus particles in the mesocosm water (determined from most probable number assays) used for clearance incubations revealed 2×10^3 (95% CI, 0.94–4.1 $\times 10^3$) viruses mL^{-1}. The proportion of infectious virus particles (most probable number : flow cytometry counts) in the water used for incubations was thus < 1%. Assuming a virus clearance rate of 3.75 mL ind^{-1} h^{-1} (Fig. 1), a starting virus concentration of 6×10^5 particles mL^{-1} (Fig. 1), an *O. dioica* defecation rate of 6 fecal pellets ind^{-1} h^{-1} (López-Urrutia and Acuña 1999), and an *O. dioica* particle ingestion efficiency of 30% (Conley and Sutherland 2017), each *O. dioica* fecal pellet may contain 1.13 $\times 10^5$ virus particles. Our most probable number results suggest that approximately 1000 (< 1% of 1.13 $\times 10^5$) of the fecal-packaged virus particles would be infectious. Considering local high densities of *O. dioica* in the ocean during the spring/summer (Båmstedt et al. 2005) when *E. huxleyi* forms enormous blooms in the upper photic zone (Tyrrell and Merico 2004) that are eventually decimated by the virus (Bratbak et al. 1993, 1995), this novel packaging mechanism for ingested virus particles has the potential to alter the ecological trajectory of a considerable fraction of *E. huxleyi* virus assemblages in the marine environment.

One study of calanoid copepod grazing on virus-infected *E. huxleyi* cells suggests that virus particles packaged into copepod fecal pellets is one mechanism regulating both the vertical and horizontal dispersal of the virus in the water column (Frada et al. 2014). One noteworthy difference between that study and the present is that host *E. huxleyi* cells in the present study were deliberately excluded from clearance incubations in order to assess the ability of *O. dioica* to remove the virus from water independent of its host. It is unclear the extent to which packaging of the virus into *O. dioica* fecal pellets represents a mechanism of vertical dispersal (viruses are transported to deeper water and/or bottom sediments) or simply a mechanism of virus loss from the marine plankton. Encounter rates of host *E. huxleyi* with fecal-packaged viruses in the water column would be diminished relative to planktonic viruses, particularly as fecal pellets sink rapidly (Dagg and Brown 2005) and fecal-packaged viruses would therefore be rapidly transported out of patches of high *E. huxleyi* density (Bratbak et al. 1993). Our demonstration that fecal-packaged viruses retain some degree of infectivity suggests that fecal-packaging can also function as a virus dispersal mechanism via sinking (Dagg and Brown 2005), in which case an investigation of the vertical distribution of the virus in areas with and without seasonal blooms of *O. dioica* might be informative. Vertically dispersed viruses that persist in the environment could seed future *E. huxleyi* infections via mixing or advection (Short 2012 and references therein), as has been suggested for viruses in freshwater lakes (Short et al. 2011) and coastal regions (Tomaru et al. 2007). Nonetheless, we cannot exclude the possibility that fecal-packaging results in significant virus loss due to digestive degradation during *O. dioica* gut passage or decay during sinking and sedimentation (Wommack and Colwell 2000), re-working by zooplankton (Koski et al. 2007), or degradation by bacteria (Turner 2002).

In addition to fecal pellets, it is also possible that virus particles trapped in discarded *O. dioica* houses experience altered ecological trajectories relative to planktonic virus particles. *O. dioica* houses may act as a dispersal agent for trapped virus particles due to their theoretically high particle retention rates (Gorsky et al. 1984; Conley and Sutherland 2017) and high house sinking rates (Troedsson et al. 2009). In our previous study (Lawrence et al. 2018), we observed that technical challenges associated with loose particle adherence (Conley et al. 2018) made the quantification of virus particles trapped in discarded *O. dioica* houses problematic. Thus, the packaging of infectious virus particles into *O. dioica* houses was not investigated during the present study. Nonetheless, virus removal by *O. dioica* and the packaging of infectious virus particles into *O. dioica* fecal pellets implicate the *O. dioica*-virus interaction as one possible regulatory mechanism driving marine virus ecological trajectories, likely through a combination of virus dispersal and virus loss. As sinking and persistence of trapped virus particles is one possible trajectory, we propose that future research should investigate marine sediments for the presence of infectious *E. huxleyi* virus particles, particularly in regions where *O. dioica* and *E. huxleyi* are known to co-occur in high abundances.

In this study, we have demonstrated that the filter-feeding appendicularian *O. dioica* is able to remove *E. huxleyi* virus from the natural viral assemblages formed during an induced *E. huxleyi* phytoplankton bloom. The presence of infectious viruses within fecal pellets and their subsequent release demonstrate that *O. dioica* fecal pellets can serve as a dispersal mechanism for this virus. The potential for *O. dioica* to remove other large viruses suggests that interactions between *O. dioica* and marine femtoplankton may represent a more general mechanism regulating virus dynamics, dispersal and persistence in the marine environment.

References

Allen, M. J., D. C. Schroeder, A. Donkin, K. J. Crawfurd, and W. H. Wilson. 2006. Genome comparison of two *Coccolithoviruses*. Virol. J. **3**: 1–6. doi:10.1186/1743-422X-3-15

Bedo, A. W., J. L. Acuna, D. Robins, and R. P. Harris. 1993. Grazing in the micron and the sub-micron particle size

range: The case of *Oikopleura dioica* (Appendicularia). Bull. Mar. Sci. **53**: 2–14.

Bolger, A. M., M. Lohse, and B. Usadel. 2014. Trimmomatic: A flexible trimmer for Illumina sequence data. Bioinformatics **30**: 2114–2120. doi:10.1093/bioinformatics/btu170

Bouquet, J. M., E. Spriet, C. Troedsson, H. Otter, D. Chourrout, and E. M. Thompson. 2009. Culture optimization for the emergent zooplanktonic model organism *Oikopleura dioica*. J. Plankton Res. **31**: 359–370. doi:10.1093/plankt/fbn132

Bratbak, G., J. K. Egge, and M. Heldal. 1993. Viral mortality of the marine alga *Emiliania huxleyi* (Haptophyceae) and termination of algal blooms. Mar. Ecol. Prog. Ser. **93**: 39–48.

Bratbak, G., M. Levasseur, S. Michaud, G. Cantin, E. Fernandez, B. R. Heimdal, and M. Heldal. 1995. Viral activity in relation to *Emiliania huxleyi* blooms: A mechanism of DMSP release? Mar. Ecol. Prog. Ser. **128**: 133–142.

Breitbart, M. 2012. Marine viruses: Truth or dare. Ann. Rev. Mar. Sci. **4**: 425–448. doi:10.1146/annurev-marine-120709-142805

Breitbart, M., C. Bonnain, K. Malki, and N. A. Sawaya. 2018. Phage puppet masters of the marine microbial realm. Nat. Microbiol. **3**: 754–766. doi:10.1038/s41564-018-0166-y

Broms, F., and P. Tiselius. 2003. Effects of temperature and body size on the clearance rate of Oikopleura dioica. J. Plankton Res. **25**: 573–577.

Brum, J. R., R. O. Schenck, and M. B. Sullivan. 2013. Global morphological analysis of marine viruses shows minimal regional variation and dominance of non-tailed viruses. ISME J. **7**: 1738–1751. doi:10.1038/ismej.2013.67

Brussaard, C. P. D., and others. 2008. Global-scale processes with a nanoscale drive: The role of marine viruses. ISME J. **2**: 575–578. doi:10.1038/ismej.2008.31

Buchfink, B., X. Chao, and D. H. Huson. 2015. Fast and sensitive protein alignment using DIAMOND. Nat. Methods **12**: 59–60. doi:10.1038/nmeth.3176

Båmstedt, U., H. J. Fyhn, M. B. Martinussen, O. Mjaavatten, and O. Grahl-Nielsen. 2005. Seasonal distribution, diversity and biochemical composition of appendicularians in Norwegian fjords, p. 227–254. *In* G. Gorsky, M. Youngbluth, and D. Deibel [eds.], Response of marine ecosystems to global change. Contemporary Publishing International.

Castberg, T., A. Larsen, R. A. Sandaa, and others. 2001. Microbial population dynamics and diversity during a bloom of the marine coccolithophorid *Emiliania huxleyi* (Haptophyta). Mar. Ecol. Prog. Ser. **221**: 39–46. doi:10.3354/meps221039

Castberg, T., R. Thyrhaug, A. Larsen, R. A. Sandaa, M. Heldal, J. L. Van Etten, and G. Bratbak. 2002. Isolation and characterization of a virus that infects *Emiliania huxleyi* (Haptophyta). J. Phycol. **38**: 767–774. doi:10.1046/j.1529-8817.2002.02015.x

Claverie, J. M., and C. Abergel. 2018. Mimiviridae: An expanding family of highly diverse large dsDNA viruses infecting a wide phylogenetic range of aquatic eukaryotes. Viruses **10**: 8–15. doi:10.3390/v10090506

Conley, K. R., and K. R. Sutherland. 2017. Particle shape impacts export and fate in the ocean through interactions with the globally abundant appendicularian *Oikopleura dioica*. PLoS One **12**: e0183105. doi:10.1371/journal.pone.0183105

Conley, K. R., B. J. Gemmell, J.-M. Bouquet, E. M. Thompson, and K. R. Sutherland. 2018. A self-cleaning biological filter: How appendicularians mechanically control particle adhesion and removal. Limnol. Oceanogr. **63**: 927–938. doi:10.1002/lno.10680

Dadon-Pilosof, A., and others. 2017. Surface properties of SAR11 bacteria facilitate grazing avoidance. Nat. Microbiol. **2**: 1608–1615. doi:10.1038/s41564-017-0030-5

Dagg, M. J., and S. L. Brown. 2005. The potential contribution of fecal pellets from the larvacean *Oikopleura dioica* to vertical flux of carbon in a river dominated coastal margin, p. 293–397. *In* G. Gorsky, M. Youngbluth, and D. Deibel [eds.], Response of marine ecosystems to global change. Contemporary Publishing International.

Deibel, D., and C. V. Powell. 1987. Comparison of the ultrastructure of the food-concentrating filter of two appendicularians. Mar. Ecol. Prog. Ser. **39**: 81–85. doi:10.3354/meps039081

Egge, J. K., and D. L. Aksnes. 1992. Silicate as regulating nutrient in phytoplankton competition. Mar. Ecol.: Prog. Ser. **83**: 281–289.

Fernández, D., Á. López-Urrutia, A. Fernández, J. L. Acuña, and R. Harris. 2004. Retention efficiency of 0.2 to 6 μm particles by the appendicularians *Oikopleura dioica* and *Fritillaria borealis*. Mar. Ecol.: Prog. Ser. **266**: 89–101. doi:10.3354/meps266089

Flood, P. R. 1978. Filter characteristics of appendicularian food catching nets. Experientia **34**: 173–175.

Frada, M. J., D. Schatz, V. Farstey, J. E. Ossolinski, H. Sabanay, S. Ben-Dor, I. Koren, and A. Vardi. 2014. Zooplankton may serve as transmission vectors for viruses infecting algal blooms in the ocean. Curr. Biol. **24**: 2592–2597. doi:10.1016/j.cub.2014.09.031

González, J. M., and C. A. Suttle. 1993. Grazing by marine nanoflagellates on viruses and virus-sized particles: Ingestion and digestion. Mar. Ecol.: Prog. Ser. **94**: 1–10.

González, H. E., S. R. González, and G. J. A. Brummer. 1994. Short-term sedimentation pattern of zooplankton, faeces and microplankton at a permanent station in the Bjørnafjorden (Norway) during April–May 1992. Mar. Ecol.: Prog. Ser. **105**: 31–45.

Gorsky, G., N. S. Fisher, and S. W. Fowler. 1984. Biogenic debris from the pelagic tunicate, *Oikopleura dioica*, and its role in the vertical transport of a transuranium element. Estuar. Coast. Shelf Sci. **18**: 13–23. doi:10.1016/0272-7714(84)90003-9

Gorsky, G., and R. Fenaux. 1998. The role of appendicularia in marine food webs, p. 161–169. *In* Q. Bone [ed.], The biology of pelagic tunicates. Oxford Univ. Press.

Hansen, F. C., H. J. Witte, and J. Passarge. 1996. Grazing in the heterotrophic dinoflagellate *Oxyrrhis marina*: Size

selectivity and preference for calcified *Emiliania huxleyi* cells. Aquat. Microb. Ecol. **10**: 307–313.

Huson, D. H., A. F. Auch, J. Qi, and S. C. Schuster. 2007. MEGAN analysis of metagenomic data. Genome Res. **17**: 377–386.

Hyatt, D., G. L. Chen, P. F. LoCascio, M. L. Land, F. W. Larimer, and L. J. Hauser. 2010. Prodigal: Prokaryotic gene recognition and translation initiation site identification. BMC Bioinf. **11**: 1–11. doi:10.1186/1471-2105-11-119

Johannessen, T. V., G. Bratbak, A. Larsen, H. Ogata, E. S. Egge, B. Edvardsen, W. Eikrem, and R. A. Sandaa. 2015. Characterization of three novel giant viruses reveals huge diversity among viruses infecting Prymnesiales (Haptophyta). Virology **476**: 180–188. doi:10.1016/j.virol.2014.12.014

Koski, M., E. F. Møller, M. Maar, and A. W. Visser. 2007. The fate of discarded appendicularian houses: Degradation by the copepod, *Microsetella norvegica*, and other agents. J. Plankton Res. **29**: 641–654. doi:10.1093/plankt/fbm046

Lawrence, J. E., A. M. Chan, and C. A. Suttle. 2002. Viruses causing lysis of the toxic bloom-forming alga *Heterosigma akashiwo* (Raphidophyceae) are widespread in coastal sediments of British Columbia, Canada. Limnol. Oceanogr. **47**: 545–550. doi:10.4319/lo.2002.47.2.0545

Lawrence, J., J. Töpper, E. Petelenz-Kurdziel, G. Bratbak, A. Larsen, E. Thompson, C. Troedsson, and J. L. Ray. 2018. Viruses on the menu: The appendicularian *Oikopleura dioica* efficiently removes viruses from seawater. Limnol. Oceanogr. **63**: S244–S253. doi:10.1002/lno.10734

Li, D., C. M. Liu, R. Luo, K. Sadakane, and T. W. Lam. 2015. MEGAHIT: An ultra-fast single-node solution for large and complex metagenomics assembly via succinct de Bruijn graph. Bioinformatics **31**: 1674–1676. doi:10.1093/bioinformatics/btv033

López-Urrutia, Á., and J. L. Acuña. 1999. Gut throughput dynamics in the appendicularian *Oikopleura dioica*. Mar. Ecol. Prog. Ser. **191**: 195–205.

MacKinder, L. C. M., and others. 2009. A unicellular algal virus, *Emiliania huxleyi* virus 86, exploits an animal-like infection strategy. J. Gen. Virol. **90**: 2306–2316. doi:10.1099/vir.0.011635-0

Marston, M. F., and others. 2012. Rapid diversification of coevolving marine *Synechococcus* and a virus. Proc. Natl. Acad. Sci. USA **109**: 4544–4549. doi:10.1073/pnas.1120310109

Martínez-Martínez, J., A. Boere, I. Gilg, J. W. M. Van Lent, H. J. Witte, J. D. L. Van Bleijswijk, and C. P. D. Brussaard. 2015. New lipid envelope-containing dsDNA virus isolates infecting *Micromonas pusilla* reveal a separate phylogenetic group. Aquat. Microb. Ecol. **74**: 17–28. doi:10.3354/ame01723

Martiny, J. B. H., L. Riemann, M. F. Marston, and M. Middelbøe. 2014. Antagonistic coevolution of marine planktonic viruses and their hosts. Ann. Rev. Mar. Sci. **6**: 393–414. doi:10.1146/annurev-marine-010213-135108

Mojica, K. D. A., and C. P. D. Brussaard. 2014. Factors affecting virus dynamics and microbial host-virus interactions in marine environments. FEMS Microbiol. Ecol. **89**: 495–515. doi:10.1111/1574-6941.12343

NCBI Resource Coordinators. 2016. Database resources of the National Center for Biotechnology Information. Nucleic Acids Res. **44**: D7–D19. doi:10.1093/nar/gkv1290

Noble, R. T., and J. A. Fuhrman. 1999. Breakdown and microbial uptake of marine viruses and other lysis products. Aquat. Microb. Ecol. **20**: 1–11. doi:10.1016/S0082-0784(67)80129-2

Pagarete, A., M. J. Allen, W. H. Wilson, S. A. Kimmance, and C. de Vargas. 2009. Host-virus shift of the sphingolipid pathway along an *Emiliania huxleyi* bloom: Survival of the fattest. Environ. Microbiol. **11**: 2840–2848. doi:10.1111/j.1462-2920.2009.02006.x

Pagarete, A., and others. 2014. Dip in the gene pool: Metagenomic survey of natural coccolithovirus communities. Virology **466–467**: 129–137. doi:10.1016/j.virol.2014.05.020

Plummer, M. 2016. rjags: Bayesian graphical models using MCMC. R package version 4–6. Available from http://CRAN.R-project.org/package5rjags

Qin, Q. W., T. J. Lam, Y. M. Sin, H. Shen, S. F. Chang, G. H. Ngoh, and C. L. Chen. 2001. Electron microscopic observations of a marine fish iridovirus isolated from brown-spotted grouper, *Epinephelus tauvina*. J. Virol. Methods **98**: 17–24.

Rao, V. C., T. G. Metcalf, and J. L. Melnick. 1986. Human viruses in sediments, sludges, and soils. Bull. World Health Organ. **64**: 1–14.

Rohwer, F., and R. V. Thurber. 2009. Viruses manipulate the marine environment. Nature **459**: 207–212. doi:10.1038/nature08060

Sandaa, R.-A., J. E. Storesund, E. Olesin, M. L. Paulsen, A. Larsen, G. Bratbak, and J. L. Ray. 2018. Seasonality drives microbial community structure, shaping both eukaryotic and prokaryotic host–viral relationships in an Arctic marine ecosystem. Viruses **10**: 1–22. doi:10.3390/v10120715

Sandaa, R. A., M. Heldal, T. Castberg, R. Thyrhaug, and G. Bratbak. 2001. Isolation and characterization of two viruses with large genome size infecting *Chrysochromulina ericina* (Prymnesiophyceae) and *Pyramimonas orientalis* (Prasinophyceae). Virology **290**: 272–280. doi:10.1006/viro.2001.1161

Sato, R., Y. Tanaka, and T. Ishimaru. 2001. House production by *Oikopleura dioica* (Tunicata, Appendicularia) under laboratory conditions. J. Plankton Res. **23**: 415–423. doi:10.1093/plankt/23.4.415

Schroeder, D. C., J. Oke, G. Malin, and W. H. Wilson. 2002. Coccolithovirus (Phycodnaviridae): Characterisation of a new large dsDNA algal virus that infects *Emiliania huxleyi*. Arch. Virol. **147**: 1685–1698. doi:10.1007/s00705-002-0841-3

Sczyrba, A., and others. 2017. Critical assessment of metagenome interpretation—A benchmark of metagenomics software. Nat. Methods **14**: 1063–1071. doi:10.1038/nmeth.4458

Short, C. M., O. Rusanova, and S. M. Short. 2011. Quantification of virus genes provides evidence for seed-bank populations of phycodnaviruses in Lake Ontario, Canada. ISME J. **5**: 810–821.

Short, S. M. 2012. The ecology of viruses that infect eukaryotic algae. Environ. Microbiol. **14**: 2253–2271. doi:10.1111/j.1462-2920.2012.02706.x

Sutherland, K. R., L. P. Madin, and R. Stocker. 2010. Filtration of submicrometer particles by pelagic tunicates. Proc. Natl. Acad. Sci. USA **107**: 15129–15134. doi:10.1073/pnas.1003599107

Tarutani, K., K. Nagasaki, and M. Yamaguchi. 2000. Viral impacts on total abundance and clonal composition of the harmful bloom-forming phytoplankton: *Heterosigma akashiwo*. Appl. Environ. Microbiol. **66**: 4916–4920. doi:10.1128/AEM.66.11.4916-4920.2000

Thingstad, T. F. 2000. Elements of a theory for the mechanisms controlling abundance, diversity, and biogeochemical role of lytic bacterial viruses in aquatic systems. Limnol. Oceanogr. **45**: 1320–1328. doi:10.4319/lo.2000.45.6.1320

Tomaru, Y., and others. 2007. Ecological dynamics of the bivalve-killing dinoflagellate *Heterocapsa circularisquama* and its infectious viruses in different locations of western Japan. Environ. Microbiol. **9**: 1376–1383.

Troedsson, C., J.-M. Bouquet, R. Skinnes, J.-L. Acuña, K. Zech, M. E. Frischer, and E. M. Thompson. 2009. Regulation of filter-feeding house components in response to varying food regimes in the appendicularian, *Oikopleura dioica*. J. Plankton Res. **31**: 1453–1463. doi:10.1093/plankt/fbp085

Troedsson, C., M. E. Frischer, J. C. Nejstgaard, and E. M. Thampson. 2007. Molecular quantification of differential ingestion and particle trapping rates by the appendicularian *Oikopleura dioica* as a function of prey size and shape. Limnol. Oceanogr. **52**: 416–427. doi:10.4319/lo.2007.52.1.0416

Tuma, R. S., M. P. Beaudet, X. Jin, L. J. Jones, C. Y. Cheung, S. Yue, and V. L. Singer. 1999. Characterization of SYBR gold nucleic acid gel stain: A dye optimized for use with 300-nm ultraviolet transilluminators. Anal. Biochem. **268**: 278–288.

Turner, J. T. 2002. Zooplankton fecal pellets, marine snow and sinking phytoplankton blooms. Aquat. Microb. Ecol. **27**: 57–102.

Tyrrell, T., and A. Merico. 2004. *Emiliania huxleyi* bloom observations and the conditions that induce them, p. 75–97. *In* H. R. Thiersten and J. R. Young [eds.], Coccolithophores from molecular processes to global impact. Springer.

Vincent, F., U. Sheyn, Z. Porat, and A. Vardi. 2020. Visualizing active viral infection reveals diverse cell fates in synchronized algal bloom demise. Proc. Natl. Acad. Sci. USA **118**: e2021586118. doi:https://doi.org/10.1073/pnas.2021586118

Welsh, J. E., P. Steenhuis, K. R. de Moraes, J. van der Meer, D. W. Thieltges, and C. P. Brussaard. 2020. Marine virus predation by non-host organisms. Sci. Rep. **10**: 1–9. doi:https://doi.org/10.1038/s41598-020-61691-y

Weinbauer, M. G., and F. Rassoulzadegan. 2004. Are viruses driving microbial diversification and diversity? Environ. Microbiol. **6**: 1–11. doi:10.1046/j.1462-2920.2003.00539.x

Wilson, W. H., J. L. Van Etten, and M. J. Allen. 2009. The Phycodnaviridae: The story of how tiny giants rule the world, p. 1–42. *In* J. L. Van Etten [ed.], Lesser known large dsDNA viruses. Springer.

Wommack, K. E., and R. R. Colwell. 2000. Virioplankton: Viruses in aquatic ecosystems. Microbiol. Mol. Biol. Rev. **64**: 69–114.

Acknowledgments

The authors express gratitude to Assaf Vardi and Daniella Schatz from the Weizmann Institute of Science for their generous access to mesocosm water, equipment, expertise, and preliminary results, without which this study would not have been possible. The authors would also like to thank the CeBiTec Center for Biotechnology Genomics Platform and Computational Metagenomics Group at Universität Bielefeld for assistance with metavirome sequencing and bioinformatic analysis. This study was funded by the Research Council of Norway project number 275710 "VIROVAC - filter-feeding mesozooplankton as uncharted accomplices in marine virus ecology." The mesocosm experiment was funded by the EU H2020 infrastructure project "AQUACOSM" (EU H2020-INFRAIA-project No 731065). J.L. was generously supported by a Harrison McCain Visitorship while on sabbatical at the University of Bergen from 2017 to 2018, and by an NSERC Discovery Grant.

Conflict of Interest

None declared.

Submitted 04 January 2021
Revised 28 May 2021
Accepted 20 August 2021

Associate editor: Tatiana Rynearson